doi.org/10.36721/PJPS.2026.39.11.306.1

Astragaloside IV attenuates high glucose-induced podocyte ferroptosis via the GSK3β/Nrf2/GPX4 pathway

Mengya Gao[1#], Hong Jiang[2#], Kangya Lei[3], Jiaqi Liu[3] and Lei Liu[1]*

[1]Department of Nephrology, The First Affiliated Hospital of Bengbu Medical University, Bengbu 233004, Anhui, China
[2]Department of Nephrology, Bengbu Hospital of Traditional Chinese Medicine, Bengbu 233080, Anhui, China
[3]Clinical College, Bengbu Medical University, Bengbu 233030, Anhui, China

Abstract: **Objectives**: To investigate whether AS-IV alleviates high glucose (HG)-induced podocyte ferroptosis and whether this effect is associated with the GSK3β/Nrf2/GPX4 axis. **Methods**: Differentiated MPC-5 podocytes were exposed to HG (30 mmol/L) with or without AS-IV, the GSK3β inhibitor LY2090314, or the ferroptosis inhibitor Ferrostatin-1 (Fer-1). An osmotic control (mannitol) was included. Cell viability was quantified with the CCK-8 assay. Levels of reactive oxygen species (ROS), malondialdehyde (MDA), glutathione (GSH) and Fe^{2+} were measured. Lipid peroxidation was detected using C11-BODIPY 581/591. Mitochondrial morphology was examined by transmission electron microscopy and protein expression was analyzed by Western blot. **Results**: HG exposure induced podocyte injury, characterized by decreased viability, increased oxidative stress (elevated ROS, MDA and lipid ROS), GSH depletion, iron overload and mitochondrial damage. The osmotic control did not reproduce these effects. AS-IV or Fer-1 significantly attenuated the HG-induced damage and lipid peroxidation. At the molecular level, HG downregulated Nephrin, p-GSK3β (Ser9), Nrf2 and GPX4, while upregulating total GSK3β. AS-IV treatment partially reversed these protein expression changes and produced a protective pattern similar to that of LY2090314. **Conclusion**: AS-IV alleviates HG-induced podocyte injury, possibly by suppressing ferroptosis and this protective effect may involve modulation of the GSK3β/Nrf2/GPX4 axis. The results offer new insights into DN pathogenesis and support AS-IV as a potential therapeutic candidate.

Keywords: Astragaloside IV; Diabetic nephropathy; Ferroptosis; GSK3β/Nrf2/GPX4 signaling pathway; Podocytes

Submitted on 08-11-2025 – Revised on 16-04-2026 – Accepted on 25-05-2026

INTRODUCTION

Diabetic nephropathy (DN) is a prevalent and severe microvascular complication of diabetes and a leading cause of end-stage renal disease (Selby and Taal, 2020; Dwivedi and Sikarwar, 2025). According to the International Diabetes Federation (IDF), the global population affected by diabetes was approximately 537 million in 2021 and is projected to reach 643 million by 2030 (Wang *et al*., 2023a; Kumar *et al*., 2024). Podocytes are crucial for maintaining the glomerular filtration barrier and their injury is a key driver of proteinuria and renal function decline in DN (Li *et al*., 2023b; Barutta *et al*., 2022). Current therapeutic strategies primarily focus on glycemic and blood pressure control (Hanna et al., 2025), underscoring the need to identify additional protective mechanisms to preserve podocyte function in DN.

Astragaloside IV (AS-IV), one of the key biologically active saponins obtained from *Astragalus membranaceus*, exhibits multifaceted therapeutic properties, including antioxidative, anti-inflammatory and anti-apoptotic activities (Liang *et al*., 2023; Zhang *et al*., 2020). Preclinical studies demonstrate its renoprotective effects in DN models, such as attenuating glomerular basement membrane thickening and mesangial expansion (Li *et al*., 2023a; Qu *et al*., 2024). Beyond renal disease, AS-IV has also been investigated in cardiovascular disorders, liver fibrosis, neurodegenerative diseases and cancer, highlighting its therapeutic versatility (Zhang *et al*., 2022; Zhang *et al*., 2020). Nevertheless, whether AS-IV mitigates high-glucose (HG)- induced podocyte injury through modulation of ferroptosis remains unknown.

Ferroptosis is characterized by iron-dependent lipid peroxidation and compromised glutathione peroxidase 4 (GPX4) function and its involvement in DN pathogenesis is increasingly recognized (Dixon *et al*., 2012; Friedmann Angeli *et al*., 2014). Hyperglycemia can promote ferroptosis in podocytes by inducing oxidative stress, glutathione depletion, and iron accumulation (Hong *et al*., 2024). The glycogen synthase kinase-3β (GSK3β)/nuclear factor erythroid 2-related factor 2 (Nrf2)/GPX4 axis represents a critical regulatory node linking cellular stress to ferroptosis defense. GSK3β activation can promote Nrf2 degradation, thereby suppressing the expression of antioxidant enzymes like GPX4 (Chowdhry *et al*., 2013; Cuadrado *et al*., 2019). Moreover, emerging evidence indicates that GSK3β can influence ferroptotic sensitivity by regulating cellular iron metabolism and iron homeostasis–related genes (Wang *et al*., 2021). Nrf2 transcriptionally regulates multiple antioxidant genes, including glutathione peroxidase 4 (GPX4), a key enzyme

**Corresponding author:* e-mail: fbqrubmfizy@hotmail.com; bbmcll@163.com
#These authors contributed equally and are the co-first authors.

that protects cells against lipid peroxidation during ferroptosis (Wang *et al*., 2023b; Ursini and Maiorino, 2020)—it is plausible that the GSK3β–Nrf2–GPX4 signaling axis mediates susceptibility to ferroptosis under diabetic stress conditions.

This study aimed to investigate whether AS-IV protects podocytes from high glucose (HG)-induced injury by suppressing ferroptosis and to explore the potential involvement of the GSK3β/Nrf2/GPX4 signaling pathway. These findings provide new mechanistic insights into the renoprotective effects of AS-IV and support the targeting of ferroptosis as a potential therapeutic strategy for DN.

MATERIALS AND METHODS

Reagents and preparation

AS-IV (purity ≥ 98%) was supplied by Aladdin (Cat# 83207-58-3). Stock solutions were freshly prepared as follows (Ma *et al*., 2024; Shen *et al*., 2023). A 0.4 mg/mL AS-IV stock solution was prepared by dissolving 0.4 mg of AS-IV in 1 mL of DMSO and a 1.2 mg/mL stock solution was prepared by dissolving 1.2 mg of AS-IV in 1 mL of DMSO. For experimental use, stock solutions were diluted into culture medium to the desired working concentrations, and the final DMSO concentration was adjusted to 0.1%. The final working concentrations of AS-IV were 20 μM (AS-IV-L) and 50 μM (AS-IV-H). These concentrations were selected based on previous *in vitro studies in podocyte and renal injury models, which have demonstrated the effective,* non-cytotoxic activity of AS-IV within the micromolar range (Ma *et al*., 2024; Shen *et al*., 2023). The ferroptosis-specific inhibitor Ferrostatin-1 (Fer-1, Cat# S7243, Selleckchem, USA) was prepared as a 10 mM stock solution in DMSO and stored at −20 °C. The working concentration of Fer-1 used in the experiments was 1 μM. The lipid peroxidation probe C11-BODIPY 581/591 (Cat# D3861, Thermo Fisher Scientific, USA) was prepared as a 2 mM stock solution in DMSO and stored at −20 °C, protected from light.

Cell culture and model establishment

Conditionally immortalized mouse podocytes (MPC-5; iCell Bioscience, Cat# iCell-m081) were used in this study. MPC-5 cells were cultured in RPMI-1640 medium (Solarbio, Cat# 10491) supplemented with 10% FBS, 100 U/mL penicillin–streptomycin and 10 U/mL recombinant mouse IFN-γ (Solarbio, Cat# P00215). Cells were maintained at 33°C in a 5% CO_2 atmosphere to preserve their proliferative state. When transferred to 37°C and cultured in the absence of IFN-γ, MPC-5 cells ceased proliferation and began differentiation, reaching maturity as podocytes after approximately 14 days. All subsequent experiments were performed using these differentiated podocytes. The high-glucose (HG) model was generated by treating cells with a 30 mmol/L glucose environment for 24 h. To rule out potential effects from increased osmolarity, an osmotic control group was established by treating cells with normal glucose medium (5.5 mM D-glucose) supplemented with 24.5 mM D-mannitol for 24 h, thereby maintaining a total osmolarity equivalent to that of the HG medium. For intervention experiments, cells were co-incubated with AS-IV or the GSK3β inhibitor LY2090314 (Aladdin, Cat#603288-22-8) for 24h. To specifically inhibit ferroptosis, cells in the designated groups were co-treated with 1 μM Fer-1 for 24 h, along with HG and/or drug treatments.

Cell viability assay

Cell viability was evaluated using the Cell Counting Kit-8(CCK-8; C0037, Guangzhou Yujia Biotechnology Co., Ltd.). MPC-5 cells were seeded into 96-well plates according to the assigned experimental groups and cultured at 37°C in 5% CO_2 for 24h. Then, each well received 10μL of CCK-8 and was incubated for 2 h. Absorbance was read on a SpectraMax i3x (Molecular Devices, USA). All assays were performed independently in triplicate.

Measurement of oxidative stress and ferroptosis-related indicators

The Reactive Oxygen Species Assay Kit (DCFH-DA, Cat# S0033S, Beyotime Biotechnology, Shanghai, China) was used to measure intracellular ROS levels. After treatment, cells were incubated with 10 μmol/L DCFH-DA at 37 °C for 20 min in the dark, washed three times with PBS and observed under a fluorescence microscope (excitation/emission = 488/525 nm). Fluorescence intensity was quantified using ImageJ to evaluate ROS production.

Malondialdehyde (MDA; Cat# S0131S, Beyotime, Shanghai), glutathione (GSH; Cat# S0053; Beyotime, Shanghai), and ferrous iron (Iron Assay Kit; Cat# ab83366; Abcam) concentrations were evaluated using commercial assay kits according to the manufacturers' guidelines.

Measurement of lipid peroxidation

Lipid peroxidation was assessed using the fluorescent probe C11-BODIPY 581/591. After the indicated treatments, cells were incubated with 2 μM C11-BODIPY 581/591 in serum-free medium at 37°C for 30 min in the dark. Subsequently, cells were washed three times with PBS. The fluorescence signals (red, excitation/emission = 581/591 nm, indicative of the reduced probe; green, excitation/emission = 488/510 nm, indicative of the oxidized probe) were captured using a fluorescence microscope (Nikon, Japan). The degree of lipid peroxidation was quantified as the ratio of green to red fluorescence intensities using Image J.

Transmission electron microscopy (TEM)

Cells were fixed in 2.5% glutaraldehyde, postfixed in 1% osmium tetroxide, dehydrated through a graded ethanol series and embedded in epoxy resin. After uranyl acetate and lead citrate staining of the ultrathin sections, mitochondrial ultrastructure was visualized using TEM.

Western blot analysis

Protein extraction was performed using RIPA buffer supplemented with protease and phosphatase inhibitors, and the extracted proteins were quantified using a BCA assay. Equal amounts of protein (30μg per lane) were separated by SDS-PAGE and transferred onto PVDF membranes. After blocking with 5% nonfat milk for 1 h, the membranes were incubated overnight at 4°C with the following primary antibodies (1:1000, Abcam): Nephrin (ab58969), GSK3β (phospho S9) (p-GSK3β, ab75814), GSK3β (ab264268), GPX4 (ab125066) and Nrf2 (ab62352). Subsequently, HRP-conjugated secondary antibody (1:5000, Abcam) was applied to the membranes and incubated for 1h at ambient temperature. Visualization of protein bands used an enhanced chemiluminescence detector (ECL; Bio-Rad, USA), and intensities were analyzed with ImageJ, with β-actin (1:5000, Abcam, ab8226) as an internal control.

Statistical analysis

Experimental procedures were replicated at least three times to confirm the robustness of the findings. Results are summarized as the mean ± standard deviation (SD). Statistical assessments were performed with IBM SPSS Statistics 23.0 (IBM Corp., Armonk, NY, USA). Two-group comparisons employed an unpaired Student's t-test, and multiple-group analyses used a one-way ANOVA with Tukey's post hoc test. A P value < 0.05 was considered statistically significant.

RESULTS

AS-IV improves podocyte viability under high-glucose conditions

AS-IV is a cycloartane-type triterpene saponin composed of a cycloastragenol aglycone bearing hydroxyl substitutions and glycosidic linkages. Its structure features a tetracyclic triterpenoid backbone with attached β-D-glucopyranosyl residues, conferring the characteristic saponin architecture (Fig. 1A). CCK-8 assay revealed that HG exposure markedly decreased podocyte viability relative to control ($P < 0.001$) (Fig. 1B). AS-IV treatment significantly restored cell viability, with the high-dose group (HG+AS-IV-H) showing a greater effect than the low-dose group (HG+AS-IV-L), although still below control ($P < 0.001$). Importantly, the reduction in cell viability was specific to high glucose, as the mannitol osmotic control group showed no significant difference compared to the normal glucose control group (Fig. S1A).

AS-IV attenuates HG-induced oxidative stress and mitochondrial damage

ROS analysis by fluorescence microscopy and quantification showed a significant increase in ROS levels after HG exposure ($P < 0.001$). In contrast, AS-IV treatment reduced ROS accumulation, with the high-dose group showing stronger inhibition ($P < 0.001$) (Fig. 2A). Consistently, MDA levels were markedly elevated in the HG group and decreased upon AS-IV treatment, with a greater reduction in the high-dose group ($P < 0.001$, Fig. 2B). Moreover, GSH levels were significantly reduced by HG stimulation. In contrast, AS-IV intervention restored intracellular antioxidant capacity, with the higher concentration yielding a more robust effect ($P < 0.05$, Fig. 2C). Consistent with this, the osmotic control group did not exhibit a significant decrease in GSH level compared to the normal control (Fig. S1B), further confirming that the oxidative stress was induced by high glucose rather than hyperosmolarity. In parallel, intracellular Fe^{2+} levels were markedly increased in the HG group and were significantly reduced by AS-IV treatment, suggesting reduced ferroptosis-related iron overload ($P < 0.05$, Fig. 2D). Transmission electron microscopy further revealed mitochondrial protection by AS-IV: control cells exhibited normal mitochondrial morphology, whereas HG treatment caused swelling and cristae disruption. AS-IV alleviated mitochondrial structural damage, with the most evident recovery in the high-dose group (Fig. 2E). To further substantiate the involvement of ferroptosis, the specific ferroptosis inhibitor Ferrostatin-1 (Fer-1) was employed, and lipid peroxidation, a key ferroptosis hallmark, was assessed. Consistent with the ferroptosis hypothesis, co-treatment with Fer-1 significantly rescued the HG-induced loss of cell viability (Fig. S2A). Moreover, using the lipid peroxidation sensor C11-BODIPY 581/591, a substantial increase in lipid ROS following HG stimulation was observed, as indicated by an elevated oxidized/reduced fluorescence ratio. This increase was markedly attenuated by both Fer-1 and AS-IV treatment (Fig. S2B). Together, the protective effect of Fer-1 and the reduction in lipid peroxidation by AS-IV further support the involvement of ferroptosis in HG-induced podocyte injury and suggest that ferroptosis suppression contributes to the protective action of AS-IV.

AS-IV alleviates HG-induced podocyte injury, an effect correlated with the modulation of the GSK3β/Nrf2/GPX4 pathway

Western blot analysis showed that HG exposure significantly reduced the protein levels of Nephrin, p-GSK3β (Ser9) and Nrf2 ($P < 0.001$) (Fig. 3A), indicating podocyte injury and impaired antioxidant defense. AS-IV treatment restored these protein levels, with stronger effects in the high-dose group (HG+AS-IV-H), approaching those in the control group.

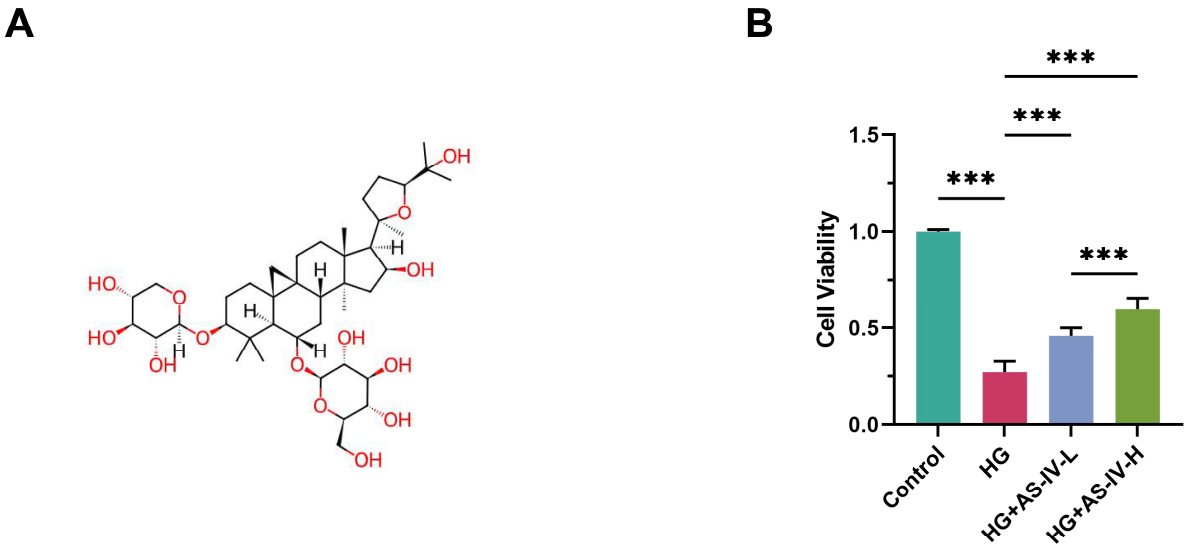

Fig. 1: Chemical structure of AS-IV and its effect on podocyte viability under HG conditions. (A) Chemical structure of AS-IV; (B) Cell viability of MPC-5 under different treatments, measured by CCK-8 assay. Results are presented as mean ± SD based on three separate experiments (n = 3). ***P < 0.001. AS-IV, astragaloside IV; HG, high-glucose; MPC-5, mouse podocytes; CCK-8, Cell Counting Kit-8.

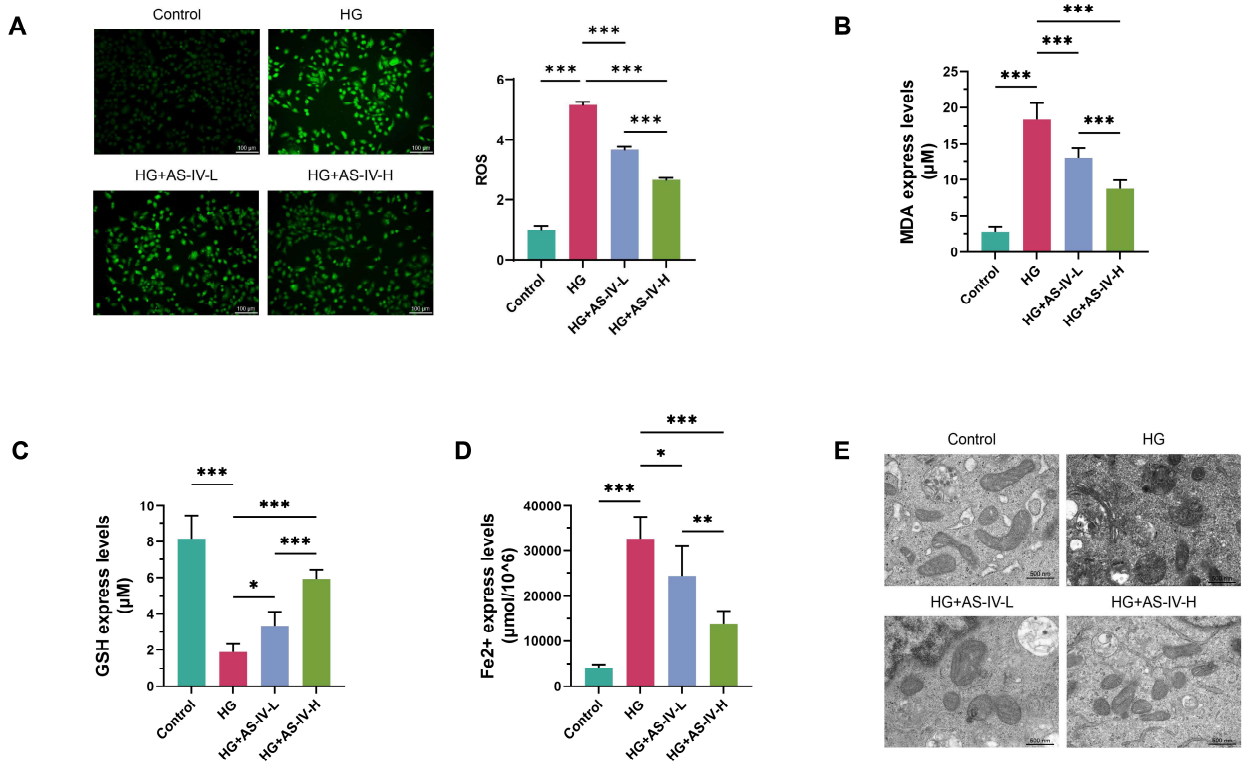

Fig. 2: AS-IV regulates oxidative stress and ferroptosis-related indicators in HG-treated podocytes. (A) Fluorescence microscopy images and quantification of ROS; (B) Intracellular MDA levels; (C) Intracellular GSH levels; (D) Intracellular Fe^{2+} levels; (E) TEM observation of mitochondrial ultrastructure. Data are expressed as mean ± SD (n = 3). *P < 0.05; **P < 0.01; ***P < 0.001; ROS, reactive oxygen species; MDA, malondialdehyde; GSH, glutathione; Fe^{2+}, ferrous iron; TEM, transmission electron microscopy.

Further analysis revealed that HG exposure significantly downregulated GPX4, Nrf2, Nephrin and p-GSK3β, while upregulating total GSK3β ($P < 0.001$) (Fig. 3B). AS-IV markedly attenuated these alterations, as reflected by increased GPX4, Nrf2, Nephrin and p-GSK3β expression and reduced total GSK3β expression.

AS-IV and GSK3β inhibition alleviate HG-induced podocyte injury

CCK-8 assay revealed that HG exposure markedly reduced podocyte viability ($P < 0.001$), indicating severe cellular injury. Remarkably, treatment with AS-IV significantly restored cell survival, with efficacy comparable to that of the GSK3β inhibitor LY2090314 (Fig. 4A). Consistent with ferroptosis-associated injury, HG exposure led to pronounced increases in intracellular ROS and MDA, accompanied by a significant depletion of GSH and excessive accumulation of Fe^{2+} ($P < 0.001$) (Fig. 4B–E). Both AS-IV and LY2090314 interventions effectively mitigated these alterations, as evidenced by reduced ROS and MDA accumulation, restoration of intracellular GSH content and attenuation of Fe^{2+} overload. TEM provided further confirmation at the ultrastructural level: podocytes exposed to HG exhibited typical ferroptosis-related mitochondrial abnormalities, including swelling, disrupted and fragmented cristae and partial cristae loss. By contrast, AS-IV and LY2090314 treatment preserved mitochondrial integrity, as evidenced by reduced swelling and relatively intact cristae morphology, resembling the structural features observed in the control group (Fig. 4F).

DISCUSSION

This study provides evidence that Astragaloside IV (AS-IV) alleviates high glucose (HG)-induced podocyte injury. Beyond the well-documented anti-inflammatory, anti-apoptotic and antifibrotic effects of AS-IV in DN, suppression of ferroptosis was identified as an additional mechanism contributing to its protective action. This protective effect may further involve modulation of the GSK3β/Nrf2/GPX4 axis, a pathway linking cellular stress signaling to the key ferroptosis defense enzyme GPX4.

Ferroptosis, driven by iron-dependent lipid peroxidation, is increasingly recognized as a pathogenic mechanism in DN (Miao *et al*., 2023; Wang *et al*., 2024). These data align with this paradigm, demonstrating that HG induces key ferroptotic features in podocytes, including lipid peroxidation, glutathione (GSH) depletion and labile iron accumulation. The protective effect of the ferroptosis inhibitor Ferrostatin-1 further supports the functional involvement of this cell death pathway. Importantly, AS-IV treatment effectively countered these changes, mitigating lipid ROS accumulation and cell death, thereby positioning ferroptosis inhibition as a plausible mechanism for its cytoprotective effect.

AS-IV, a principal bioactive saponin molecule sourced from Astragalus membranaceus, demonstrates a broad range of biological effects, including antioxidative, anti-inflammatory, anti-apoptotic and antifibrotic functions (Liang *et al*., 2023). In DN models, AS-IV has been reported to reduce mesangial expansion, attenuate glomerular basement membrane thickening and suppress oxidative stress (Commission *et al*., 2023). The present study extends this understanding by showing that AS-IV suppresses ferroptosis in HG-exposed podocytes, highlighting a previously underexplored aspect of its renoprotective action. Direct evidence was obtained that AS-IV mitigates HG-induced podocyte ferroptosis, thereby expanding the current understanding of its renoprotective mechanisms. These results complement previous work by identifying ferroptosis inhibition as an additional layer of AS-IV-mediated protection, alongside its established effects on inflammation, apoptosis and fibrosis.

Given the known multi-faceted pharmacological profile of AS-IV, which includes anti-apoptotic and anti-inflammatory effects, the possibility of concurrent modulation of other regulated cell death pathways (e.g., apoptosis, necroptosis, or pyroptosis) under high-glucose conditions cannot be entirely excluded (Hu *et al*., 2024; Leng *et al*., 2019; Zhang *et al*., 2022). The primary objective of the present study, however, was to investigate the novel role of ferroptosis and its regulation by AS-IV, a mechanism that has recently garnered substantial interest in DN pathogenesis (Deng *et al*., 2023; Liu *et al*., 2024). The specificity of ferroptosis involvement in the present model is supported by two key observations: first, the significant cytoprotection afforded by the specific ferroptosis inhibitor Fer-1 (Guo *et al*., 2022; Liu *et al*., 2020) and second, the direct attenuation by AS-IV of high glucose-induced lipid peroxidation, a hallmark of ferroptosis, as detected by C11-BODIPY 581/591 (Huang *et al*., 2025; Zhang *et al*., 2025). While these data strongly implicate ferroptosis inhibition as a key mechanism of AS-IV's action, future studies that comprehensively assess markers of apoptosis, necroptosis, and pyroptosis in parallel are warranted to delineate the potential contributions and hierarchy of these cell death pathways in this context.

Mechanistically, the GSK3β/Nrf2/GPX4 axis appears to participate importantly in this process. Nrf2 serves as a master transcription factor that regulates cellular antioxidant capacity and ferroptosis resistance by activating downstream genes, such as GPX4, which prevents lipid peroxidation. Dysregulation of this pathway has been implicated in ferroptosis across multiple disease models (Yan *et al*., 2023). GSK3β, a serine/threonine kinase, promotes Nrf2 degradation via ubiquitination, thereby weakening antioxidant defenses and predisposing cells to ferroptosis (Cahuzac *et al*., 2023).

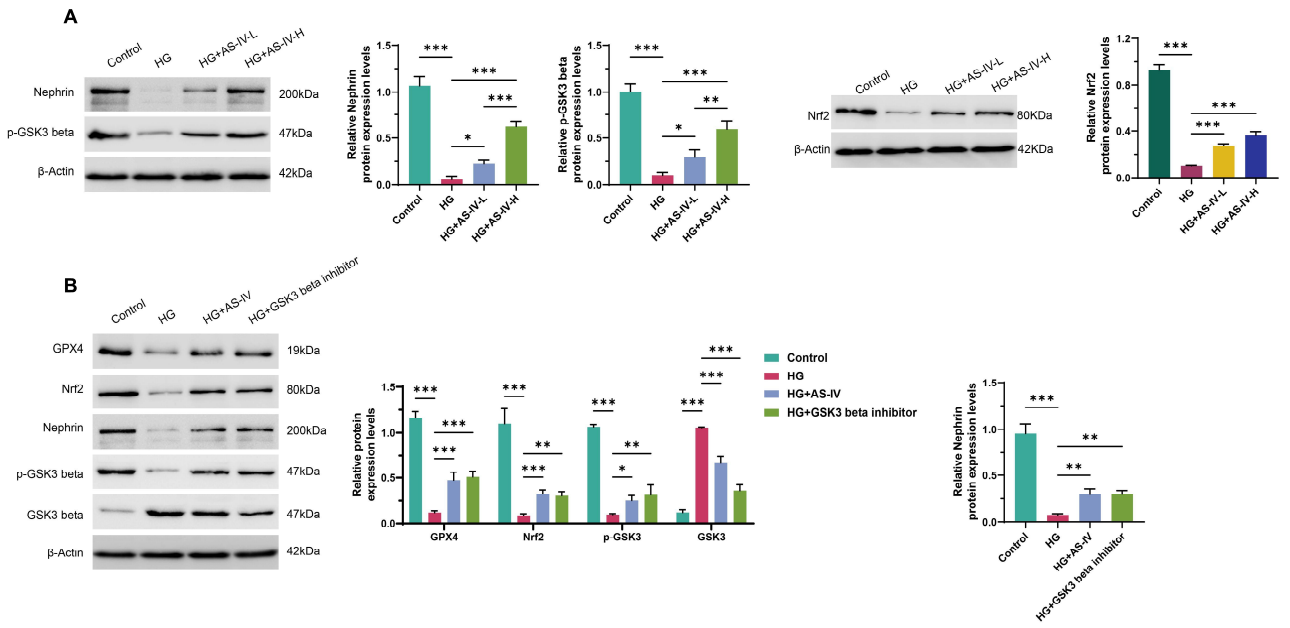

Fig. 3: AS-IV modulates key podocyte protein expression, possibly via the GSK3β/Nrf2/GPX4 signaling pathway. (A) Western blot analysis and quantification of Nephrin, p-GSK3β, and Nrf2; (B) Western blot and quantification of GPX4, Nrf2, Nephrin, p-GSK3β and GSK3β. Data are expressed as mean ± SD (n = 3). *P < 0.05; **P < 0.01; ***P < 0.001. GPX4, glutathione peroxidase 4; GSK3β, glycogen synthase kinase 3β; Nrf2, nuclear factor erythroid 2-related factor 2.

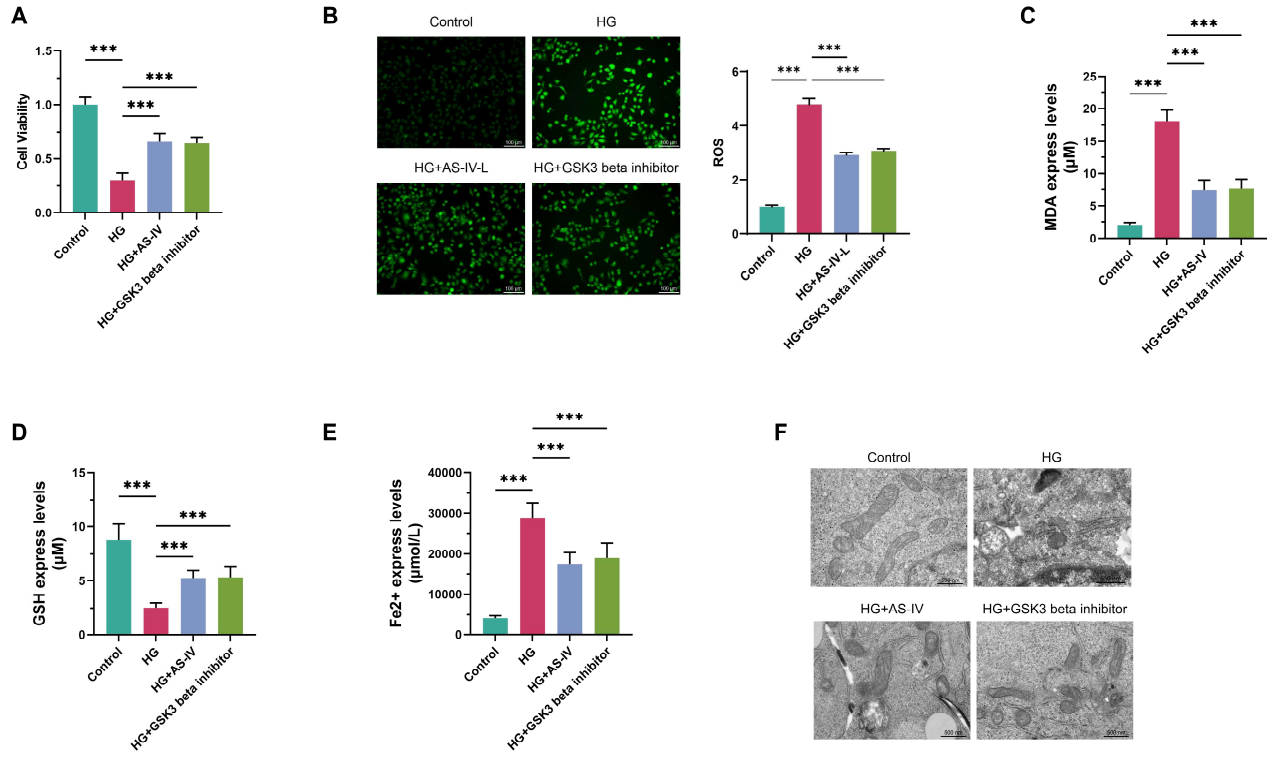

Fig. 4: Effects of AS-IV and GSK3β inhibition on HG-induced podocyte injury. (A) Cell viability of MPC-5 podocytes measured by CCK-8 assay; (B) ROS fluorescence microscopy and quantification; (C) MDA levels; (D) GSH levels; (E) Fe^{2+} levels; (F) TEM images of mitochondrial ultrastructure. Data are expressed as mean ± SD (n = 3). ***P < 0.001.

In this study, high glucose activated GSK3β, reduced its phosphorylation and suppressed Nrf2 and GPX4 expression, while AS-IV treatment reversed these changes, showing effects similar to pharmacological GSK3β inhibition (Fig. S3). These results suggest that the protective effect of AS-IV is associated with attenuation of ferroptosis and correlates with modulation of the GSK3β/Nrf2/GPX4 axis in podocytes under high-glucose conditions. This mechanistic insight aligns with previous studies in cardiovascular and neurodegenerative diseases, further extending its relevance to DN.

From a clinical standpoint, ferroptosis has become an attractive therapeutic target in DN and other kidney diseases (Yang *et al*., 2023). Current treatment strategies primarily focus on glycemic and blood pressure control, which delay but do not prevent podocyte injury. AS-IV, as a natural compound with multi-target pharmacological activities, represent a promising approach to address this unmet need. By inhibiting ferroptosis, AS-IV not only enhances podocyte survival but also provides a novel dimension of renoprotection beyond conventional therapies (Hu *et al*., 2024). Moreover, its favorable safety profile and long-standing use in traditional Chinese medicine support its translational potential as a candidate therapy for DN.

Nevertheless, this study has several limitations. First, regarding mechanistic evidence, the conclusions of the present study are primarily based on correlative protein expression data and pharmacological inhibition. Definitive genetic evidence (e.g., using siRNA) to establish the necessity of the GSK3β/Nrf2/GPX4 axis and direct assessment of Nrf2 nuclear translocation or GPX4 enzymatic activity, are required for future validation. The potential off-target effects of the inhibitor LY2090314 also necessitate confirmation through genetic means. Second, concerning the research model and clinical translation, the findings are derived from an *in-vitro* podocyte monoculture system, which, while ideal for dissecting cell-autonomous mechanisms, does not recapitulate the multicellular interactions of the diabetic glomerulus and lacks *in-vivo* validation. Furthermore, the *in-vivo* achievability of the effective AS-IV concentrations used here, the potential contribution of other regulated cell death pathways (e.g., apoptosis) and comprehensive pharmacokinetic and safety profiles remain to be evaluated. These issues should be addressed in future studies to better evaluate the therapeutic potential of AS-IV for clinical translation.

CONCLUSION

This study reveals that AS-IV can mitigate high glucose-induced podocyte damage. Importantly, it provides new evidence that AS-IV's protective action may involve reducing ferroptotic activity via modulation of the GSK3β/Nrf2/GPX4 signaling axis. These findings provide additional insight into the mechanisms of podocyte injury in DN and support further investigation of AS-IV as a potential therapeutic candidate.

Acknowledgments
None.

Authors' contributions
Mengya Gao and Hong Jiang: Contributed equally to this work, performed the experiments and drafted the manuscript; Kangya Lei and Jiaqi Liu: Responsible for data collection and analysis; Lei Liu: Conceived and designed the study, supervised the project and revised the manuscript. All authors read and approved the final manuscript.

Funding
There was no funding.

Data availability statement
The datasets generated and/or analysed during the current study are available from the corresponding author upon reasonable request.

Ethical approval
Ethical approval was not required for this study because only commercially available established cell lines were used, and no human participants or experimental animals were involved.

Conflict of interest
The authors declare no conflict of interest.

REFERENCES

Barutta F, Bellini S and Gruden G (2022). Mechanisms of podocyte injury and implications for diabetic nephropathy. *Clin Sci (Lond)*, **136**(7): 493-520.

Cahuzac KM, Lubin A, Bosch K, Stokes N, Shoenfeld SM, Zhou R, Lemon H, Asara J and Parsons RE (2023). AKT activation because of PTEN loss upregulates xCT via GSK3β/NRF2, leading to inhibition of ferroptosis in PTEN-mutant tumor cells. *Cell Rep*, **42**(5): 112536.

Chowdhry S, Zhang Y, McMahon M, Sutherland C, Cuadrado A and Hayes JD (2013). Nrf2 is controlled by two distinct β-TrCP recognition motifs in its Neh6 domain, one of which can be modulated by GSK-3 activity. *Oncogene*, **32**(32): 3765-3781.

Commission NH, Education Mo, Affairs MoC, Finance Mo, Administration NHS, Medicine NAoTC, Administration NCfDCaPNMP, Unions A-CFoT and Societies A-CFoWs (2023). Action plan for accelerating the elimination of cervical cancer (2023-2030). *Chin J Viral Dis.*, **13**(4): 243-244.

Cuadrado A, Rojo AI, Wells G, Hayes JD, Cousin SP, Rumsey WL, Attucks OC, Franklin S, Levonen A-L and Kensler TW (2019). Therapeutic targeting of the NRF2 and KEAP1 partnership in chronic diseases. *Nature reviews Drug discovery*, **18**(4): 295-317.

Deng Q, Zhu Y, Zhang M, Fei A, Liang J, Zheng J, Zhang Q, Cheng T and Ge X (2023). Ferroptosis as a potential new therapeutic target for diabetes and its complications. *Endocr Connect*, **12**(3): e220419.

Dixon SJ, Lemberg KM, Lamprecht MR, Skouta R, Zaitsev EM, Gleason CE, Patel DN, Bauer AJ, Cantley AM, Yang WS, Morrison B, 3rd and Stockwell BR (2012). Ferroptosis: An iron-dependent form of nonapoptotic cell death. *Cell*, **149**(5): 1060-72.

Dwivedi S and Sikarwar MS (2025). Diabetic nephropathy: Pathogenesis, mechanisms and therapeutic strategies. *Horm Metab Res*, **57**(1): 7-17.

Friedmann Angeli JP, Schneider M, Proneth B, Tyurina YY, Tyurin VA, Hammond VJ, Herbach N, Aichler M, Walch A, Eggenhofer E, Basavarajappa D, Radmark O, Kobayashi S, Seibt T, Beck H, Neff F, Esposito I, Wanke R, Forster H, Yefremova O, Heinrichmeyer M, Bornkamm GW, Geissler EK, Thomas SB, Stockwell BR, O'Donnell VB, Kagan VE, Schick JA and Conrad M (2014). Inactivation of the ferroptosis regulator Gpx4 triggers acute renal failure in mice. *Nat Cell Biol*, **16**(12): 1180-91.

Guo M, Zhu Y, Shi Y, Meng X, Dong X, Zhang H, Wang X, Du M and Yan H (2022). Inhibition of ferroptosis promotes retina ganglion cell survival in experimental optic neuropathies. *Redox Biol*, **58**: 102541.

Hong J, Li X, Hao Y, Xu H, Yu L, Meng Z, Zhang J and Zhu M (2024). The PRMT6/STAT1/ACSL1 axis promotes ferroptosis in diabetic nephropathy. *Cell Death Differ*, **31**(11): 1561-1575.

Hu Z, Zhou Y, Gao C, Liu J, Pan C and Guo J (2024). Astragaloside IV attenuates podocyte apoptosis via regulating TXNIP/NLRP3/GSDMD signaling pathway in diabetic nephropathy. *Diabetol Metab Syndr*, **16**(1): 296.

Huang G, Cai Y, Ren M, Zhang X, Fu Y, Cheng R, Wang Y, Miao M, Zhu L and Yan T (2025). Salidroside sensitizes Triple-negative breast cancer to ferroptosis by SCD1-mediated lipogenesis and NCOA4-mediated ferritinophagy. *J Adv Res*, **74**: 589-607.

Kumar A, Gangwar R, Zargar AA, Kumar R and Sharma A (2024). Prevalence of diabetes in India: A review of IDF diabetes atlas 10th edition. *Curr Diabetes Rev*, **20**(1): e130423215752.

Leng B, Zhang Y, Liu X, Zhang Z, Liu Y, Wang H and Lu M (2019). Astragaloside IV suppresses high glucose-induced NLRP3 inflammasome activation by inhibiting TLR4/NF-kappaB and CaSR. *Mediators Inflamm*, **2019**: 1082497.

Li L, Zhang Y, Luo Y, Meng X, Pan G, Zhang H, Li Y and Zhang B (2023). The molecular basis of the anti-inflammatory property of astragaloside IV for the treatment of diabetes and its complications. *Drug Des Devel Ther*, **17**: 771-790.

Li X, Zhang Y, Xing X, Li M, Liu Y, Xu A and Zhang J (2023). Podocyte injury of diabetic nephropathy: Novel mechanism discovery and therapeutic prospects. *Biomed Pharmacother*, **168**: 115670.

Liang Y, Chen B, Liang D, Quan X, Gu R, Meng Z, Gan H, Wu Z, Sun Y, Liu S and Dou G (2023). Pharmacological effects of astragaloside IV: A review. *Molecules*, **28**(16): 6118.

Liu J, Ren J, Zhou L, Tan K, Du D, Xu L, Cao W and Zhang Y (2024). Proteomic and lipidomic analysis of the mechanism underlying astragaloside IV in mitigating ferroptosis through hypoxia-inducible factor 1alpha/heme oxygenase 1 pathway in renal tubular epithelial cells in diabetic kidney disease. *J Ethnopharmacol*, **334**: 118517.

Liu P, Feng Y, Li H, Chen X, Wang G, Xu S, Li Y and Zhao L (2020). Ferrostatin-1 alleviates lipopolysaccharide-induced acute lung injury via inhibiting ferroptosis. *Cell Mol Biol Lett*, **25**: 10.

Ma Y, Hu Y, Ruan Y, Jiang X, Zhao M, Wang Y, Ke Y, Shi M and Lu G (2024). Astragaloside IV relieves passive heymann nephritis and podocyte injury by suppressing the TRAF6/NF-κb axis. *Ren Fail*, **46**(2): 2371992.

Miao R, Fang X, Zhang Y, Wei J, Zhang Y and Tian J (2023). Iron metabolism and ferroptosis in type 2 diabetes mellitus and complications: Mechanisms and therapeutic opportunities. *Cell Death Dis*, **14**(3): 186.

Qu C, Tan X, Hu Q, Tang J, Wang Y, He C, He Z, Li B, Fu X and Du Q (2024). A systematic review of astragaloside IV effects on animal models of diabetes mellitus and its complications. *Heliyon*, **10**(5): e26863.

Selby NM and Taal MW (2020). An updated overview of diabetic nephropathy: Diagnosis, prognosis, treatment goals and latest guidelines. *Diabetes Obes Metab*, **22**(Suppl 1): 3-15.

Shen Q, Fang J, Guo H, Su X, Zhu B, Yao X, Wang Y, Cao A, Wang H and Wang L (2023). Astragaloside IV attenuates podocyte apoptosis through ameliorating mitochondrial dysfunction by up-regulated Nrf2-ARE/TFAM signaling in diabetic kidney disease. *Free Radic Biol Med*, **203**: 45-57.

Ursini F and Maiorino M (2020). Lipid peroxidation and ferroptosis: the role of GSH and GPx4. *Free Radical Biology and Medicine*, **152**: 175-185.

Wang H, Yu X, Liu D, Qiao Y, Huo J, Pan S, Zhou L, Wang R, Feng Q and Liu Z (2024). VDR activation attenuates renal tubular epithelial cell ferroptosis by regulating Nrf2/HO-1 signaling pathway in diabetic nephropathy. *Adv Sci (Weinh)*, **11**(10): e2305563.

Wang L, Ouyang S, Li B, Wu H and Wang F (2021). GSK-3β manipulates ferroptosis sensitivity by dominating iron homeostasis. *Cell Death Discov.*, **7**(1): 334.

Wang W, Ji Q, Ran X, Li C, Kuang H, Yu X, Fang H, Yang J, Liu J, Xue Y, Feng B, Lei M and Zhu D (2023).

Prevalence and risk factors of diabetic peripheral neuropathy: A population-based cross-sectional study in China. *Diabetes Metab Res Rev*, **39**(8): e3702.

Wang X, Zhu W, Xing M, Zhu H, Chen E and Zhou J (2023). Matrine disrupts Nrf2/GPX4 antioxidant system and promotes hepatocyte ferroptosis. *Chem.-Biol. Interact.*, **384**: 110713.

Yan R, Lin B, Jin W, Tang L, Hu S and Cai R (2023). NRF2, a superstar of ferroptosis. *Antioxidants (Basel)*, **12**(9): 1739.

Yang C, Zhang Z, Liu J, Chen P, Li J, Shu H, Chu Y and Li L (2023). Research progress on multiple cell death pathways of podocytes in diabetic kidney disease. *Mol Med*, **29**(1): 135.

Zhang J, Wu C, Gao L, Du G and Qin X (2020). Astragaloside IV derived from Astragalus membranaceus: A research review on the pharmacological effects. *Adv Pharmacol*, **87**: 89-112.

Zhang L, Liu X, Wang J, Li Z, Wang S, Yang W, Hai Y and Liu D (2025). Kaempferol protects against doxorubicin-induced myocardial damage by inhibiting mitochondrial ROS-dependent ferroptosis. *Redox Rep*, **30**(1): 2503130.

Zhang X, Qu H, Yang T, Liu Q and Zhou H (2022). Astragaloside IV attenuate MI-induced myocardial fibrosis and cardiac remodeling by inhibiting ROS/caspase-1/GSDMD signaling pathway. *Cell Cycle*, **21**(21): 2309-2322.